Phenomenological renormalization group for cellular automata

1992 J. Phys. A: Math. Gen. 25 L1071

(http://iopscience.iop.org/0305-4470/25/17/010)

J. Phys. A: Math. Gen. 25 (1992) L1071-L1077. Printed in the UK

LETTER TO THE EDITOR

Phenomenological renormalization group for cellular automata

F Bagnoli†‖, R Bulajich‡¶, R Livi‡‖ and A Maritan§

† Dipartimento di Matematica Applicata, Università di Firenze, Via S Marta 3, I-50139 Firenze, Italy

‡ Dipartimento di Fisica, Università di Firenze, Largo E Fermi 2, I-50125 Firenze, Italy

§ Dipartimento di Fisica, Università di Padova, Via Marzolo 8, I-35131 Padova, Italy

‖ Sezione INFN and Unità INFM di Firenze, Firenze, Italy

Received 25 June 1992

Abstract. The phenomenological renormalization group method introduced by Barber for equilibrium spin models is extended to stochastic cellular automata exhibiting continuous phase transitions from a quiescent state to an active one. The method is applied to the Domany-Kinzel model, which contains bond and site directed percolation in 1+1 dimensions as special cases. A new universality class with critical exponents close to, but definitely different from, the ones of directed percolation is predicted. Finite-size scaling analysis and Monte Carlo simulations provide further support to this result.

Non-equilibrium continuous phase transitions from an active phase to a unique absorbing state characterize a wide class of dynamical models dealing with contact processes. Despite their usually simple definition in terms of local irreversible evolution rules, these models, also known as *interacting particle systems* [1], are hardly solvable. Apart from a few exact results in 1+1 dimensions [2] a variety of techniques, ranging from series analysis [3], Monte Carlo methods [4-6] to field-theoretic renormalization group [7-10], have been applied to obtain critical exponents and phase diagrams.

All the results obtained in 1+1 dimensions seem to provide strong support to the conjecture [4, 6, 10] that all these systems belong to the unique universality class of Reggeon field theory. In particular, their critical behaviour is expected to exhibit a continuous phase transition from an asymptotic absorbing state (*quiescent* phase) to an *active* phase. This suggests that renormalization group methods may be appropriate tools to face this kind of problem.

In this letter we propose an extension to probabilistic cellular automata of the phenomenological renormalization group (PRG) originally proposed by Barber [11] for multiparameter equilibrium statistical models. This method is a consequence of the finite-size properties of the correlation length.

Directed phenomena are usually modelled by local Markov processes on a regular spacetime lattice Λ, where the time axis plays the role of a privileged direction. We indicate with r and t the space and time coordinates on Λ; the vector $\boldsymbol{k}$ represents the set of parameters of the model. We define the distance of $\boldsymbol{k}$ from the critical surface S in parameter space as $\varepsilon(\boldsymbol{k}) = \inf_{\boldsymbol{k}_c \in S} |\boldsymbol{k} - \boldsymbol{k}_c|$. The difficulty of applying renormalization group methods to these models is that the correlation length ξ scales asymmetrically

¶ On sabbatical leave from Departamento de Matemáticas, Facultad de Ciencias, Universidad Nacional Autónoma de México, 04510 México DF, Mexico.

0305-4470/92/171071+07$04.50

with respect to spatial ($\xi_\perp \sim \varepsilon^{-\nu_\perp}$) and temporal ($\xi_\parallel \sim \varepsilon^{-\nu_\parallel}$) directions [12]. Asymmetric scaling factors can be avoided if the system can be considered infinite in some direction. The transfer-matrix approach studied by Kinzel [13] considers the asymptotic behaviour of spatially finite systems, so that the scaling exponent $\nu_\perp$ is related to the spatial correlation length.

We propose to consider spatially infinite systems, and to apply the PRG to *finite-time* quantities.

We need to identify the scaling properties near the critical surface of some suitable observable. For instance, good candidates for directed percolation are the scaling functions studied in [4]. For this purpose, let us point our attention on the scaling properties of the spacetime correlation function $C(r, t, \varepsilon)$, which is proportional to the probability of having an active site in r at time t, given an initial condition with only one active site in the origin; ε represents a measure of the distance in parameter space from the critical surface.

Assuming homogeneity properties of $C(r, t, \varepsilon)$ around $\varepsilon = 0$ we can write

$$C(r, t, \varepsilon) = b^{z\eta - d} C\left(\frac{r}{b}, \frac{t}{b^z}, b^{1/\nu_\perp}\varepsilon\right) \tag{1}$$

where d is the space dimension, b is the space scaling factor, η is the exponent associated with the average number of active sites at the critical surface and $z = \nu_\parallel / \nu_\perp$.

From a practical point of view it is more convenient to study the scaling behaviour of suitable observables derived from $C(r, t, \varepsilon)$, e.g.

$$n(t, \varepsilon) = \sum_r C(r, t, \varepsilon)$$

which satisfies the scaling relation

$$n(t, \varepsilon) = l^\eta n\left(\frac{t}{l}, l^{1/\nu_\parallel}\varepsilon\right) \tag{2}$$

where $l = b^z$.

As shown in [4], this function allows a good determination of the critical point for directed percolation. Moreover, regarding Monte Carlo simulations, it has better statistical properties than any other function studied in the literature [4-6].

If the model contains m parameters, the PRG transformation is defined by the map

$$\boldsymbol{k}' = R_{l,t}(\boldsymbol{k}) \tag{3}$$

which can be expressed implicitly through a set of m equations imposing the scaling invariance of $n(t, \varepsilon(\boldsymbol{k}))$,

$$\frac{n(t_i/l, \varepsilon(\boldsymbol{k}'))}{n(t_{i+1}/l, \varepsilon(\boldsymbol{k}'))} = \frac{n(t_i, \varepsilon(\boldsymbol{k}))}{n(t_{i+1}, \varepsilon(\boldsymbol{k}))} \qquad i = 1, \ldots, m \tag{4}$$

with $t_i > t_{i+1}$. This set of equations is solved for fixed $\boldsymbol{k}$ and t_i, obtaining the values of $\boldsymbol{k}'$.

In general the PRG is expected to approximate better and better the phase diagram as t_{m+1} increases, while it should not depend significantly on the choice of l.

We apply this method to the Domany-Kinzel model [2, 13], which is the simplest version of directed phenomena in $1+1$ dimensions. The model is defined on a tilted square lattice. The active (quiescent) state is represented by the symbol 1 (0). In the

language of interacting particle systems the local evolution rule is defined by the transition probabilities

$$\tau(0,0\to 1)=0$$
$$\tau(0,1\to 1)=\tau(1,0\to 1)=p$$
$$\tau(1,1\to 1)=q$$
$$\tau(x,y\to 0)=1-\tau(x,y\to 1)\qquad x,y=0,1.$$

The usual directed percolation corresponds to $q=p$ for the site problem and to $q=p(2-p)$ for the bond problem. The model can be solved exactly on the line $q=1$ [2, 13]. We have also proved that an exact solution can be obtained on the line $q=2p$, where $n(t)=(2p)^t$; the critical point at $p=\frac{1}{2}$ is characterized by mean-field critical exponents $\eta=0$ and $\nu_\parallel=1$.

Since the model depends on two parameters, the PRG *requires the calculation of* the function n for six different values of t_i. We have used a modified version of an algorithm proposed in [14]: due to the left/right symmetry of the model the algorithm allows to compute $n(t,\varepsilon(\boldsymbol{k}))$ applying the transfer matrix method to a configuration of size $t/2$. The function $n(t_i,\varepsilon(\boldsymbol{k}))$ has been calculated up to $t_1\equiv T=36$, which corresponds to a maximum cluster of 630 sites. We have chosen t_i-t_{i+1} equal to the minimum value such that t_i/l is an integer for any i.

The critical line and the fixed points of the PRG flow (3) are obtained by solving numerically equation (4) in p and q. The complete bifurcation diagram for $T=24$ and $l=2$ is reported in figure 1. In the following we shall make reference to the notations introduced in this figure, where H_1, H_2 and R are the upper hyperbolic, lower hyperbolic and fully unstable fixed points, respectively.

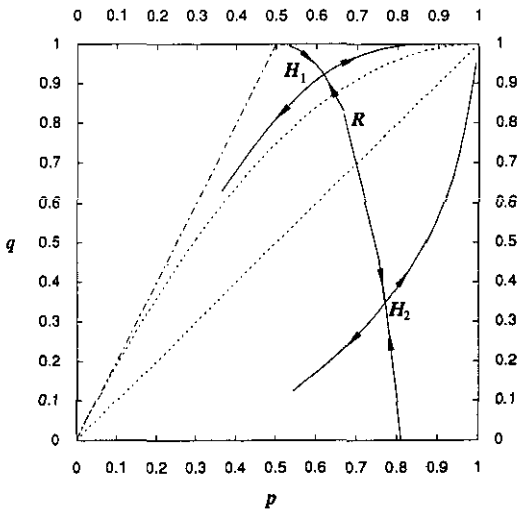

Figure 1. Phase diagram and PRG flow for $T=24$ and $l=2$. H_1 and H_2 are the hyperbolic fixed points, and R is the unstable fixed point. The model is solvable on the lines $q=1$ and $q=2p$ (dot-dashed) which are natural boundaries for the PRG flow. The upper dashed curve and the lower dashed line correspond to the bond and site percolation problems, respectively. It is worth recalling that, at variance with this picture, for $T\geqslant 44$ the bond percolation critical point belongs to the basin of attraction of H_2, i.e. R has shifted above the upper dashed curve.

The exponent η is computed by the scaling relation (2), while the exponent $\nu_\parallel$ is obtained by linearizing the map (3) in the vicinity of the hyperbolic fixed points. The coordinates of the fixed points and the corresponding exponents are reported in table 1 for different values of T and l.

Table 1. Results for the PRG fixed points and exponents for various T and l. The algorithm fails for some renormalization schemes (dashes). The estimated errors are of the order of unity on the last digit.

		H_1				H_2				R	
T	l	p	q	η	$\nu_\parallel$	p	q	η	$\nu_\parallel$	p	q
20	$\frac{4}{3}$	0.618	0.919	0.333	1.783	—	—	—	—	0.665	0.840
21	$\frac{3}{2}$	0.618	0.921	0.334	1.783	0.783	0.253	0.315	1.732	0.660	0.838
24	2	0.618	0.922	0.334	1.785	0.777	0.308	0.317	1.745	0.669	0.827
24	$\frac{3}{2}$	0.616	0.925	0.334	1.783	0.783	0.258	0.315	1.741	0.656	0.850
24	$\frac{4}{3}$	0.615	0.925	0.332	1.779	0.783	0.259	0.315	1.739	0.654	0.856
24	$\frac{6}{5}$	0.617	0.922	0.333	1.784	0.783	0.256	0.315	1.739	0.655	0.853
25	$\frac{5}{4}$	0.617	0.925	0.332	1.780	0.784	0.249	0.315	1.736	0.652	0.860
28	2	0.615	0.926	0.333	1.783	0.776	0.308	0.317	1.745	0.661	0.840
30	$\frac{3}{2}$	0.6113	0.9311	0.3313	1.7825	0.7939	0.1569	0.3127	1.7392	—	—
32	2	0.6124	0.9297	0.3317	1.7787	0.7818	0.2687	0.3152	1.7356	0.655	0.854
36	2	0.6099	0.9328	0.3306	1.7760	0.7858	0.2325	0.3137	1.7313	0.648	0.861

The qualitative features of the phase diagram in figure 1 do not change as T and l are varied. Both the critical line and the critical exponents show a very weak dependence on T and l, while the location of the fixed points seem to depend more significantly on these parameters. Actually, as T increases, H_1 and R slightly shift towards the unstable (mean field) fixed point $p=\frac{1}{2}$, $q=1$.

The PRG predicts the existence of two universality classes with different critical exponents. Their values are so close that a cross-over phenomenon could have been easily underestimated in Monte Carlo and series analysis.

Up to $T=36$ the site and bond percolation problems appear to belong to different universality classes. This scenario contrasts with the results reported in the literature [3]. In order to obtain a more accurate prediction about the universality class of the bond percolation, we followed one step of the PRG flow starting from the critical point of this model with larger values of T. For $T=40$ the flow tends towards H_1, while for $T=44$ the bond percolation problem is mapped towards H_2, i.e. it belongs to the same universality class of the site problem. It is reasonable to conjecture that this remains true as T is further increased.

The analysis of the PRG flow near R appears quite difficult because, independently of T and l, the eigenvalue corresponding to the eigendirection transverse to the critical line is very close to 1, i.e. a *marginal* case. This suggests the existence of a line of fixed points crossing the critical line at R. Anyway, our numerical analysis does not allow any conclusion on this point. Nevertheless, it would be interesting to calculate the critical exponents associated with R, which represents a third universality class in itself. It is possible that analysing an extended parameter space, R acquires one or more attractive eigendirections associated with its domain of attraction.

We have checked the PRG scenario by means of finite-size scaling analysis [15] and Monte Carlo simulations [4–6].

Regarding the former method we have exploited the scaling relation (2) in order to evaluate the critical exponents and p_c for any q at finite T. More precisely, we have computed the value of $p_c \equiv p_c(T, q)$ satisfying the equation

$$\frac{\log n(T, p_c)/n(T-1, p_c)}{\log T/(T-1)} = \frac{\log n(T-1, p_c)/n(T-2, p_c)}{\log (T-1)/(T-2)}. \tag{5}$$

For this solution both sides of this equation give the corresponding value of $\eta(T, q)$.

The plots of the resulting critical lines $p_c(T, q)$ and $\eta(T, q)$ for different values of T are reported in figures 2 and 3, respectively. As shown in figure 2, the critical line is quickly approached as T increases, except near $q = 0$ where, moreover, the distance

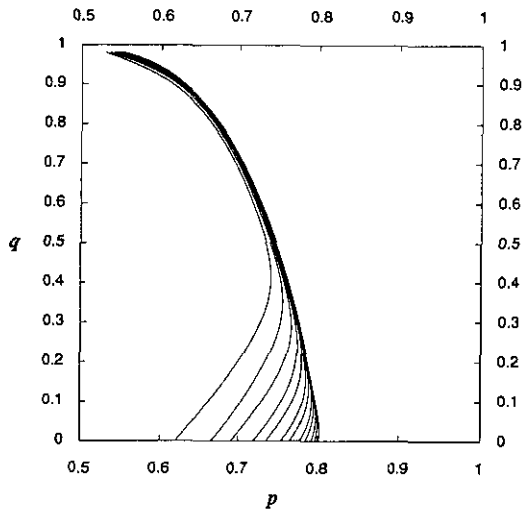

Figure 2. The critical line $p_c(T, q)$ from equation (5) for $T = 8, 10, \ldots, 30$ from left to right.

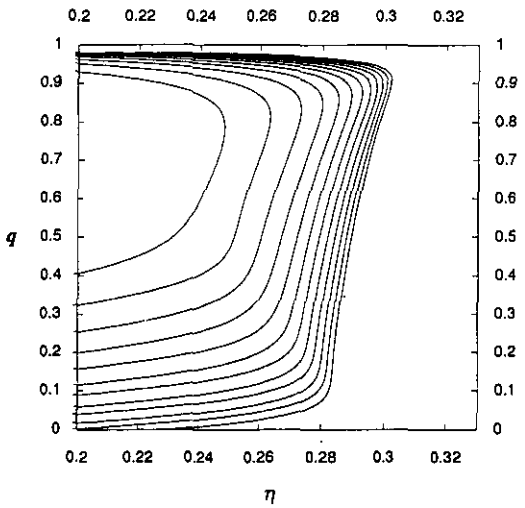

Figure 3. The exponent $\eta(T, q)$ versus q from equation (5) for $T = 8, 10, \ldots, 30$ from left to right.

between successive approximations does not decrease monotonically. Looking at figure 3, one can infer the presence of the two hyperbolic fixed points from the behaviour of $\eta(T, q)$. In fact, the hyperbolic fixed points are in correspondence with the faster convergence of the exponent η to its two different asymptotic values. For $q \to 1$, η rapidly converges to its mean-field value $\eta = 0$.

Following the suggestions of [16] we can improve this method by conjecturing that first-order corrections to finite-size scaling for $p_c(T, q)$ are expressed by

$$p_c(T, q) \simeq p_c(\infty, q) - At^{-\chi(T,q)}$$

with

$$\chi(T, q) \simeq \left[\log\left(\frac{p_c(T, q) - p_c(T-2, q)}{p_c(T-2, q) - p_c(T-4, q)} \right) \Big/ \log\left(\frac{T-2}{T} \right) \right] - 1. \tag{6}$$

In figure 4 we plot this function against q for different values of T. In the spirit of PRG, the intersections of the curves locate the hyperbolic fixed points H_1 and H_2. Notice that H_1 uniformly approaches its asymptotic values. On the contrary H_2 shows a more irregular behaviour. This effect was also present in the results reported in table 1. Anyway, the values of χ at the two fixed points are manifestly different.

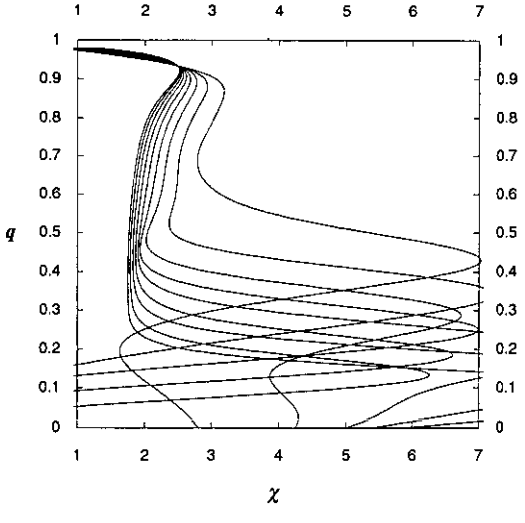

Figure 4. The exponent χ defined in equation (6) versus q for different T.

Monte Carlo simulations allow a further independent check of the presence of the two universality classes by direct computation of critical exponents. We have calculated the exponents η, δ and z related to the mean number of active sites $n(t) \sim t^{\eta}$, to the survival probability $P(t) \sim t^{-\delta}$ and to the mean radius of the active region $R(t) \sim t^{1/z}$, respectively. We have performed the simulations for $q = 0.925$ (i.e. near H_1), $q = p(2-p)$ (bond percolation), $q = p$ (site percolation) and $q = 0.25$ (i.e. close to H_2). We have averaged over 6×10^4 runs, up to time $T = 10\,000$.

The results confirm that the bond and site percolation problems do belong to the universality class of H_2 for which $\eta = 0.314(1)$, $\delta = 0.160(5)$ and $z = 1.58(1)$, while for $q = 0.925$ we have found $p_c = 0.614\,70(5)$, $\eta = 0.330(2)$, $\delta = 0.152(2)$ and $z = 1.60(2)$. The figures in parentheses indicate the uncertainty on the last digit.

Extensions of our PRG method to include a third independent critical exponent and/or a third parameter (e.g. the 'external field' $h = \tau(0, 0 \to 1)$) and applications to (2+1)-dimensional cellular automata will be the subject of future investigations.

We acknowledge useful discussions with B Derrida, M Droz and S Ruffo. Three of us (FB, RL and AM) thank ISI in Turin for its kind hospitality during the workshop *Evolution and Complexity 1991*, where this work progressed significantly. RB thanks CONACYT and DGAPA-UNAM of Mexico for partial financial support.

References

[1] Liggett T M 1985 *Interacting Particle Systems* (Berlin: Springer)
[2] Domany E and Kinzel W 1984 *Phys. Rev. Lett.* **53** 311
[3] Essam J W, Guttmann A J and De'Bell K 1988 *J. Phys. A: Math. Gen.* **21** 3815
[4] Grassberger P 1989 *J. Phys. A: Math. Gen.* **22** 3673
[5] Dickman R 1990 *Phys. Rev.* A **42** 6985
[6] Jensen I 1992 *Phys. Rev.* A **45** R563
[7] Janssen H K 1981 *Z. Phys.* B **42** 151
[8] Janssen H K 1985 *Z. Phys.* B **58** 311
[9] Grassberger P 1982 *Z. Phys.* B **47** 365
[10] Grinstein G, Lai Z W and Browne D A 1981 *Phys. Rev.* A **40** 4820
[11] Barber M N 1983 *Phys. Rev.* B **27** 5879
[12] Kamphorst Leal da Silva J and Droz M 1987 *J. Phys. A: Math. Gen.* **20** 1865
[13] Kinzel W 1985 *Z. Phys.* B **58** 229
[14] Blease J 1977 *J. Phys. C: Solid State Phys.* **10** 3461
[15] Fisher M E 1972 *Proc. 1970 Enrico Fermi Summer School, Course No 51, Varenna, Italy* (New York: Academic)
[16] Nightingale P 1982 *J. Appl. Phys.* **53** 7927